

MG-GCN: Scalable Multi-GPU GCN Training Framework

Muhammed Fatih Balin^{*†}

Kaan Sancak^{*†}

Ümit V. Çatalyürek^{‡‡}

{balin, kaan, umit}@gatech.edu

Abstract

Full batch training of Graph Convolutional Network (GCN) models is not feasible on a single GPU for large graphs containing tens of millions of vertices or more. Recent work has shown that, for the graphs used in the machine learning community, communication becomes a bottleneck and scaling is blocked outside of the single machine regime. Thus, we propose MG-GCN, a multi-GPU GCN training framework taking advantage of the high-speed communication links between the GPUs present in multi-GPU systems. MG-GCN employs multiple High-Performance Computing optimizations, including efficient re-use of memory buffers to reduce the memory footprint of training GNN models, as well as communication and computation overlap. These optimizations enable execution on larger datasets, that generally do not fit into memory of a single GPU in state-of-the-art implementations. Furthermore, they contribute to achieve superior speedup compared to the state-of-the-art. For example, MG-GCN achieves super-linear speedup with respect to DGL, on the Reddit graph on both DGX-1 (V100) and DGX-A100.

1 Introduction

Graphs are essential data-structures that can represent a variety of information, therefore they surface in many different contexts and disciplines. The Graph Convolutional Network (GCN) model is a type of Graph Neural Network (GNN) which is a very powerful graph embedding method for semi-supervised learning to solve graph representation learning problems [21, 30]. GNNs take advantage of the connectivity information presented in the graph, thus they provide flexibility and greater applicability compared to CNN models where the neighborhood structure of nodes is fixed, hence the model is more restricted. The common use cases of GNN models include *node prediction* [21] which predicts the properties of certain vertices, *graph prediction* [40] which predicts the properties of the whole

graph, and *link prediction* [39] which predicts whether there is an edge exists between two nodes. In this work, we will focus on node prediction, but our methods are extendable to graph and link prediction as well.

While training GNNs, the memory requirement for large graphs can exceed the memory capacity of a single accelerator. *Mini-batch* training is a common technique to overcome this problem to reduce the working set by creating a mini-batch of vertex samples to train the model. Consequently, it reduces the memory requirement during training. However, mini-batch training might lead to important problems. First, starting from the mini-batch nodes, it is possible to reach almost every single node in the graph in just a few hops, also known as neighborhood explosion phenomenon, which increases the work performed during a single epoch exponentially. Second, it has been shown that mini-batch training can lead to lower accuracy compared to full-batch training [17]. In this work, we focus on full-batch training on multi-GPU systems.

A major challenge to full-batch GCN training is their parallelization and scalability. The challenge stems mainly from the irregular structure of the graph which leads to load imbalance and communication cost when training on multiple GPUs. GCN has many underlying kernels, however, one of the most time consuming part is the Sparse Matrix-Dense Matrix Multiplications (SpMM). Alternative solutions are proposed to improve the performance of SpMM, such as reordering and better suited graph storage schemes and computation kernels [18].

Most of the existing systems, such as Deep Graph Learning Library (DGL), lack the support for multi-GPU training [35]. One needs to implement the parallelism manually while using DGL. DistDGL is an extension of DGL that enables multi-GPU training, however, it does not provide full-batch training, rather it uses mini-batch training [41]. Recently, ROC [17] has been proposed and it supports automatic multi-GPU GCN full-batch training on a single machine, and scales up to multiple machines. CAGNET [32] builds on top of ROC by providing distributed algorithms with different communication patterns. In their work, authors investigate different partitioning strategies to reduce the communication cost and scale up-to hundreds of GPUs. However, their results show that none of the proposed algorithms is able to scale beyond a single node (4 GPUs), primarily due to re-

^{*}Equal contribution

[†]School of Computational Science and Engineering, Georgia Institute of Technology, Atlanta, Georgia, USA

[‡]Amazon Web Services. This publication describes work performed at the Georgia Institute of Technology and is not associated with Amazon.

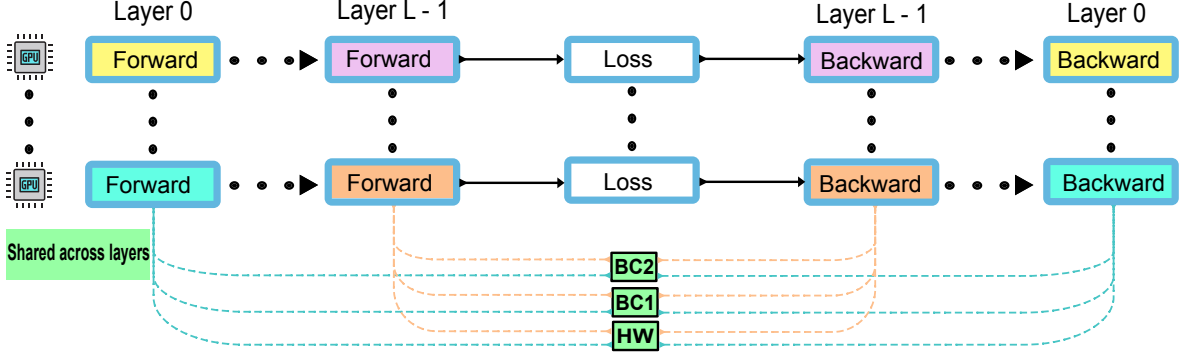


Figure 1: **Computation diagram** of an L -layer GCN model with shared buffers across layers. $BC1$: broadcast buffer, $BC2$: broadcast buffer for overlapping, HW : temporary result buffer between SpMM and GeMM.

stricted bandwidth of the available interconnect between nodes in the cluster.

In this work, we provide a framework for training GCNs on multiple GPUs that takes advantage of the high-speed communication links present in today’s multi-GPU systems [25]. We address the load imbalance problem by using simple random permutation strategy, and hide the communication by overlapping it with computation. Moreover, we carefully examine the dependency scheme of the buffers used during training and investigate ways to reduce memory requirement for GCN models to fit larger datasets into our target machines. Our optimization techniques are generalizable and can be applied to other frameworks but for reproducibility, we also release our customizable implementation of MG-GCN, as an open-source library.

2 Background

The inputs for a GCN $f_A(X)$ are the feature matrix $X \in \mathbb{R}^{n \times d}$ and the adjacency matrix $A \in \mathbb{R}^{n \times n}$, when there are n input instances and each input instance has d dimensional feature vectors. GCNs are useful when the input instances come equipped with a relation, which is represented in matrix format as A . Typically, input instances have features along them which make up X . To do learning on such a dataset, one can ignore A and fit a model that treats each input instance independently using a multi-layer perceptron. In contrast, GCNs utilize A , and instead of processing each input instance separately, it processes an input instance together with its k -hop neighborhood. Having access to an instance’s neighborhood increases the expressiveness of the model, hence aids performance immensely. As an example, consider guessing which movies an individual would like to watch. It might prove to be a hard task if we have access to a single individual. However, if we consider a group of individuals that are related to the person of interest, then the prediction task becomes much simpler as individual variance vanishes whereas group difference becomes more

visible when one looks at whole groups at once. This is why GCN often perform much better compared to simple multi-layer perceptron models that do not take into account the relations of instances [21].

The simplest variant of a GCN $f_A(H)$ with a single layer can be represented as

$$f_A(H) = \sigma(\hat{A}^T HW) \quad (1)$$

$$\hat{A}_{uv} = \frac{A_{uv}}{\sum_{w \in \mathcal{N}_i(v)} A_{wv}} \quad (2)$$

where $\mathcal{N}_i(v)$ is the set of in-edges for vertex v and σ is an element-wise nonlinear activation function, ReLU [28] in our case. Using f_A , we can construct deeper GCNs as follows for any number of layers L :

$$H^{(0)} = X \quad (3)$$

$$\vdots$$

$$H^{(L)} = f_A(H^{(L-1)}) \quad (4)$$

As depicted in Figure 1, L -layer GCN model training is composed to L forwarded passes followed by L backward passes. More specifically, given input matrix H , the operations in the forward pass of a single GCN layer can be broken down as follows:

$$HW = H * W \quad (5)$$

$$AHW = \hat{A}^T * HW \quad (6)$$

$$H' = \sigma(AHW) \quad (7)$$

where $*$ denotes the matrix multiplication operation. Similarly given the gradient from the next layer H'_G , the backward layer can be broken down as follows:

$$AHW_G = \sigma'(H'_G, AHW) \quad (8)$$

$$HW_G = \hat{A} * AHW_G \quad (9)$$

$$W_G = HW_G^T * H \quad (10)$$

$$H_G = HW_G * W^T \quad (11)$$

where we use subscript G in U_G , to denote the derivative of U with respect to the loss function.

As we will experimentally verify in Section 6.2, at the core of these GCN computations, there are two operations which are computationally the most expensive: 1) Sparse Matrix-dense Matrix multiplications (SpMM) in $\hat{A}^T * HW$ and $\hat{A} * AHW_G$, and 2) (General) dense Matrix-Matrix multiplication (GeMM) operations, in HW , $HW_G * W^T$ and $HW_G^T * H$. For efficient parallel and distributed execution, one needs to pay attention to these two operations.

3 Related Work

The growing size and scale of data encouraged many researchers to develop parallel/distributed algorithms and systems for Deep Neural Networks [2, 24]. Broadly, DNN parallelism can be generalized under 3 categories: data parallelism, model parallelism, and pipelining. Data parallelism can be further divided into 2 categories. Mini-batch parallelism creates batches from the dataset by using sampling methods, and then partitions the batches among compute resources [12, 14], while Coarse- and Fine-Grained or full-batch parallelism divides the dataset among the compute resources [38, 43]. On the other hand, model parallelism divides the model itself, and partitions the work depending on the neurons in each layer [6, 9]. Alternatively, pipelining can be achieved in two ways. Either overlapping the computations between consecutive layers, or partitioning the model according to its depth, and dividing layers among processors [1, 4, 8, 29]. Also, there has been hybrid approaches that combine multiple parallelism schemes [23].

While alternative methods exist, most of the research on GNN parallelism is focused on data parallelism, since the models are relatively simple compared to the traditional DNN models. Similar to DNNs, data parallelism can be achieved in two ways. Mini-batch, or sampling, based approaches create batches via neighborhood sampling [3, 5]. After batches are created, they are assigned to CPUs or GPUs. However, in the case of graphs, mini-batching might result in neighborhood explosion in just few hops, increasing the work performed in an epoch exponentially. Alternatively, to avoid the computation waste, one can apply full-batch parallelism where the parallelism achieved by distributing the workload among CPUs/GPUs while keeping execution order of the layers identical to the sequential method [27, 32]. In full-batch training, the model takes the whole graph and the corresponding features as input, and to achieve any parallelism one has to apply ideas similar to the model parallelism in general DNNs since the work of individual layers has to be partitioned. In this work, we focus on this aspect of GNN model training.

Most of the CPU-based systems are focused on mini-batching based methods. AliGraph is a comprehensive distributed GNN training framework that provides aggrega-

tors and operators for various GNN models [42]. AliGraph enables 4 different partitioning algorithms: METIS, Vertex cut & Edge Cut, 2D partitioning, and Streaming-style partitioning. However, it neither provides much details on the subject nor includes any scaling experiments. DistDGL [41] is a framework based on DGL that uses METIS partitioning [19]. It keeps vertex and edge features in a distributed key-value store, which can be queried during the training. DistDGL shows scaling results on the largest available benchmark datasets. However, none of these frameworks provides support for training on the full-graph. DistGNN [27] is a scalable distributed training framework for large-scale GNNs that is an extension of DGL. Unlike other frameworks, DistGNN trains the models on the full graph. It uses a vertex-cut partitioning called Libra [37], and shows substantial scaling on largest available benchmark datasets. However, as we will show in the later sections, by applying extensive memory optimizations, we are able to fit some of the largest datasets using only 1 to 8 GPUs, while achieving 12.5x faster runtimes than DistGNN’s best performance which is achieved with up to 128 sockets.

There has been various frameworks and algorithms proposed for training GNNs on GPUs. Deep Graph Library (DGL) [35] is a well-known library for implementing general GNN models. DGL provides the API for sparse matrix operations and sampling functions to implement various GNN models efficiently. Moreover, it can use Tensorflow [1], PyTorch [29] or MXNet [4] as backends for wide adoption. NeuGraph [26] is a single node multi-GPU mini-batch GNN training framework. NeuGraph introduces a programming model for GNN computations that is similar to vertex-centric programming model [13]. ROC [17] is a distributed multi-GPU GNN training framework utilizing graph partitioning via an online regression model and it proposes memory management optimizations for transfers of data between the CPU and GPU. ROC shows scalability on some of the available benchmark datasets such as Reddit and Amazon, and also it is able to do full-batch training of more complex models and achieve higher accuracy compared to sampling approaches. However, we are not able to compare with ROC, since they do not provide multi-gpu results in their work and the available code does not work as expected. CAGNET [32], inspired by the SUMMA algorithm [33], implements 1D, 1.5D, 2D and 3D partitioning strategies for full-batch training in order to reduce the communication cost. Additionally, authors provide a complexity analysis for each strategy. However, CAGNET fails to scale beyond a single node (4 GPUs) in terms of runtime performance due to the available bandwidth and the intra and inter communication topologies. Moreover, CAGNET does not have an effort to reuse memory buffers, and it relies on PyTorch and PyTorch Geometric libraries [10]. As we will show in the later sections, by adapting extensive memory optimizations, we are able to fit much larger

graphs into our target machines.

4 MG-GCN

Looking at a single layer of a GCN model particularly, we can express it via the following:

$$H^{(l+1)} = f_A(H^{(l)}) = \sigma(\hat{A}^T H^{(l)} W^{(l)}) \quad (12)$$

where matrices A , H , and W are defined in Section 2. That is, one layer of GCN consists of two main operations. For the forward propagation, first, we need to perform a Generalized Matrix Matrix Multiplication (GeMM) between the dense matrices H and W , then we need to perform a Sparse Matrix-Dense Matrix Multiplication (SpMM) between the transpose sparse matrix A , and the resulting matrix of GeMM. Later the result of SpMM is fed into a nonlinear activation function. In the backward pass, same operations are performed with the non-transposed normalized adjacency matrix \hat{A} . In the rest of this section, we will focus on the forward pass and we refer to \hat{A}^T simply as A .

In addition to our analytical analysis, we have experimentally identified the most computationally expensive kernels in GCN computation. As we will demonstrate in Section 6.2, we have profiled our single GPU GCN training with nvprof to analyze the run-time of our kernels and pinpoint the bottleneck kernels. We have observed that up to 94% of the runtime was spent during the execution of the forward and backward SpMM kernels. Therefore, we have first focused on efficient parallelization of SpMM kernel on multi-GPU setting. Moving into multi-GPU from single GPU, one needs to find ways to distribute the data into multiple GPUs, and adapt algorithms to perform parallel SpMM.

4.1 Partitioning

Given a matrix A , we can define 2D tiling (partitioning) of the matrix using two partition vectors p and q , such that p represents the partition vector of the first dimension, and q represents the partition vector of the second dimension. A partition vector p with P parts is defined as:

$$p \in \mathbb{N}^{P+1}, 0 = p(0) \leq \dots \leq p(i) \leq \dots \leq p(P) = n \quad (13)$$

Then, let us define A^{ij} as the (i, j) -th tile of the matrix.

$$p(i) \leq u < p(i+1), q(j) \leq v < q(j+1) \quad (14)$$

$$A^{ij}(u, v) = A(u + p(i), v + q(j)), u, v \in \mathbb{N} \quad (15)$$

One way to partition A , H and W is to apply symmetric partitioning, so that $p = q$, to the sparse matrix A , and then assign the tiles of A to GPUs using 1D or 2D distribution. Let's start with 1D column distribution where j -th tile column of A , A^{ij} , is assigned to j -th GPU. Moreover, we will partition dense matrix H , using 1D

partitioning by rows, with the same partition vector p , and assign H^i to i -th GPU. Likewise, the resulting dense matrix will be conformally partitioned by its rows. After partitioning, SpMM can be performed in multiple stages. In each stage, one set of rows of the result matrix can be filled, thus taking the algorithm P steps to perform, where P is the number of GPUs. Each GPU performs an SpMM with their local portions in the sparse and dense matrices. That is, at stage i , A^{ij} will be multiplied by H^j by j -th GPU, then partial results will be reduced at GPU i .

$$C^i = \sum_j A^{ij} H^j$$

The only communication needed for this operation is the reduction at the end. In this scheme, W is replicated across GPUs and is reduced at the end of every epoch of training. The reduction of W however is much faster than the communication done for the feature matrix H because of their size difference $\mathcal{O}(d^2)$ vs $\mathcal{O}(nd)$.

Alternatively, one can do 1D row distribution and assigns i -th tile row of A , A^{ij} , to i -th GPU, see Figure 2. Then, at stage i , i -th GPU broadcasts H^i , then A^{ij} will be multiplied by H^j on j -th GPU. The only communication needed for this operation is the broadcast at the beginning, see Figure 3.

$$C^i = C^i + A^{ij} H^j$$

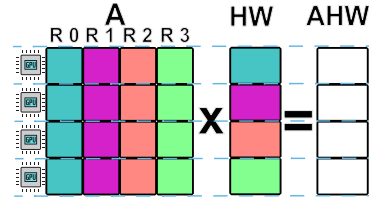


Figure 2: Partitioning of the sparse and dense matrices involved in SpMM. Colors represent stages, rows represent GPUs.

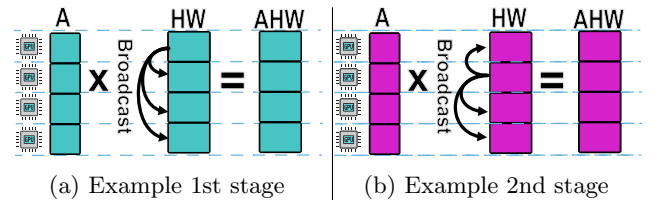


Figure 3: Example two stages of SpMM

Both of the above approaches partition H by its rows, so one might consider how it would work if H was partitioned by its columns, into $1 \times P$ tiles. For this case, let us use a partition vector p with P parts and a partition vector q with only a single part to partition A . Then, we can assign A^{i1} to i -th GPU, H^{1j} to j -th GPU. Likewise, this operation can be performed in multiple stages. At stage i ,

i -th GPU broadcasts A^{i1} , then A^{i1} will be multiplied by H^{1j} at j -th GPU. The results are kept at the j -th GPU. The only communication needed for this operation is the broadcast of the sparse matrix at the beginning.

$$C^{ij} = A^{i1} H^{1j}$$

However, for this particular partitioning strategy, there is more communication involved during the GEMM kernel. In particular since H is 1D column-partitioned, $C^{ij} \times W^{jk}$ requires a reduction over j . This means not only A is communicated, but also the dense matrix C is communicated which makes this solution undesirable. Compared to the first solution, solution 2 provides better load balance regardless of the matrix ordering, since each GPU is using the same set of rows broadcasted at each stage, the sparsity pattern of the sparse matrix will be identical across the GPUs. Nevertheless, since communication is the main bottleneck, we decide to use the broadcast variant of solution 1, as in Figure 2.

We don't discuss anymore complicated partitioning strategies such as 1.5D, 2D or 3D as we will explain the reasoning in Section 5.1. Furthermore, note that the GeMM computations on the row-partitioned feature matrices do not require any synchronization as each GPU can compute $H^i W$ in (5) independently. The element-wise activation function is also fully independent, each GPU computes it for their portions.

4.2 Memory Optimizations

To reduce memory requirements, we reuse memory buffers in the forward and backward passes, as much as possible.

In the forward and backward computations in eqs. (5) to (7), we will have a temporary result buffer called HW_B and a result buffer called AHW_B do the following mapping:

$$HW \rightarrow HW_B \quad (16)$$

$$AHW \rightarrow AHW_B \quad (17)$$

$$H' \rightarrow AHW_B \quad (18)$$

And in the backward computations in eqs. (8) to (11):

$$AHW_G \rightarrow AHW_B \quad (19)$$

$$HW_G \rightarrow HW_B \quad (20)$$

$$H_G \rightarrow AHW_B \quad (21)$$

Fig. 4a shows the mappings of the buffers for the forward computation and Fig. 4b for the backward propagation.

Notice that, each layer only requires a *single buffer* to store their output. They also use a temporary buffer that is shared across layers. Hence, each layer only increases the memory use by a single buffer, compared to $4x$ or $6x$ in other deep learning frameworks that allocates buffers for the output of SpMM, GeMM and the activation functions. Considering the backward pass adds up-to 6 buffers per

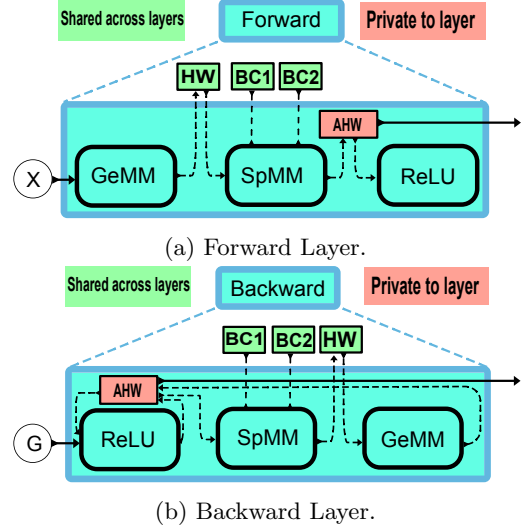


Figure 4: Forward and backward layers. Buffers are color according to being shared or private to layers. $BC1$, $BC2$, and HW are explained in Figure 1. AHW : Buffer for result of the layer.

layer in total, as shown in Fig. 1. For L -layer GCN, the total number of buffers is $L + 3$, whose sizes on average are $n \times d$.

4.3 Overlapping Computation and Communication

Each round of our multi-round SpMM is composed of a broadcast of a tile of H and a SpMM computation with a tile of A with the received tile of H . Notice that, there is an opportunity to overlap communication and computation in such a multi-round scheme. After the broadcast of first tile of H , we overlap communication of the next (remaining) tile(s) of H with the SpMM computations. In order to do that, we need an extra communication buffer for the *next* H tile. Since each GPU *keeps* its own H tile, and receives the H^i in the i -th round, each GPU needs one more extra buffer for the broadcast primitive. In total, overlapping communication and computation would require two additional buffers. In order to fully utilize communication computation overlap, we use two GPU streams: one for communication (stream 1) and one computation (stream 0). We launch all communication and computation kernels asynchronously on those two streams and wait for i -th broadcast to finish on stream 1 before we start on i -th SpMM computation on stream 0 and the $i + 1$ -th broadcast waits for the $i - 1$ -th SpMM to finish not to overwrite its input when it is ongoing.

4.4 Order of Computation and Saving one SpMM

For computing AHW , we change the order of SpMM and GeMM operations depending on the feature dimension of

the current layer $d^{(l)}$ and the next layer $d^{(l+1)}$ as allowed by associativity. If $d^{(l)} < d^{(l+1)}$, then doing SpMM, otherwise running GeMM is faster.

If the gradients all the way back to the input features are not required, then it is possible to skip the SpMM in the first layer during the backward pass. The reason is that, SpMM scales each feature dimension independently so it is possible to replace it with a diagonal feature scaling matrix in the first layer’s backward pass. In our case, each node takes the average of their neighbors, thus the identity matrix is the scaling matrix, making it a no-operation. Thus we avoid the SpMM of the first layer in the backward pass.

5 Design Decisions

5.1 Choice of the Partitioning Strategy

The communication topology of the system directly effects observed bandwidth of different communication patterns. This is clearly not an issue for systems like DGX-A100 where 8 GPU of the system are connected shared NVlink switch with 12 links, and could achieve full communication bandwidth between any pair of GPUs. Whereas, in DGX-1 there are only 6 links and connections between GPUs are asymmetric. Such asymmetry will make some theoretically optimum algorithms perform poorly on that system, since the underlying communication assumptions are not valid on that system. For example, 1.5D algorithm presented in [32] halves the theoretical communication volume, by using more memory with replication factor $c = 2$. If we group the GPUs into two groups as per the replication factor, each group has 4 links available. Then the broadcast can be faster by a factor of $\frac{6}{4 \times 2}$ in the 1.5D case. However, the last reduction among the two groups has access to only 2 links. Then, if we sum up the time required for communication for the 1.5D case, which necessitates two rounds of broadcast followed by a concurrent reduction (see [32] for the details of the algorithm) we get: $2 \frac{nd}{4 \times 4l} + \frac{nd}{4 \times 2l} = \frac{nd}{4l}$, where l is the single NVlink bandwidth. In comparison, the 1D algorithm only takes $8 \frac{nd}{8 \times 6l} = \frac{nd}{6l}$ time. On the other hand, in DGX-A100 all broadcasts and reductions can utilize all of the 12 links. Hence, summing up time required for the 1.5D algorithm, we get: $2 \frac{nd}{4 \times 12l} + \frac{nd}{4 \times 12l} = \frac{nd}{16l}$. In comparison, the 1D algorithm takes $8 \frac{nd}{8 \times 12l} = \frac{nd}{12l}$ time.

According to the above analysis, 1.5D algorithm is slower on DGX-1 by a factor of $\frac{2}{3}$ but it is faster on DGX A100 by $\frac{4}{3}$, but also requires twice as much memory. Since GNN training is usually bound by the GPU memory, we chose to implement only the 1D version.

5.2 Permutation

In order to balance the number of nonzeros in each part A^{ij} in the uniformly partitioned sparse matrices, we ran-

domly permute their vertices. This has a significant effect on load balance compared to using the original orderings of the sparse matrices which can have highly imbalanced parts. Later in Section 6.3, we show how this permutation improves the execution time with better load balancing, especially with larger number of GPUs.

6 Experimental Evaluation

6.1 Experiment Setup

Hardware and Software: We perform our experiments on two machines: NVIDIA DGX-1, also referred to as DGX-V100, and NVIDIA DGX-A100. DGX-V100 has 8 Nvidia V100 GPUs, each equipped with 32GB memory with a 900 GB/s memory bandwidth. Each V100 has 6 NVLink connections, each consisting of 2 sub-links that send data in one direction, and has a 25GB/s bandwidth. That is, each link is capable of 50GB/s bidirectional bandwidth, and theoretically, the aggregate system bandwidth is 300 GB/s. The DGX-1 is equipped with a dual 20-core Intel Xeon E5-2698 CPU with 512 GB RAM. NVIDIA DGX-A100 has 8 NVIDIA A100 GPUs, each equipped with 80GB memory with a 2 TB/s memory bandwidth. Each A100 has 12 NVLink connections, thus twice as much the bandwidth of V100. Unlike the V100, each A100 is connected to an NWSwitch, enabling a full peer-to-peer bidirectional bandwidth of 600 GB/s between any two GPUs. DGX-A100 is equipped with a dual 64-core AMD Rome 7742 CPU with 2 TB RAM. Both machines run Ubuntu 20.04.

We implemented MG-GCN using C++ standard 20 and compiled with GCC 9.3.0 and CUDA 11.4. We used CUDA’s cuSPARSE for SpMM calls with the Compressed Sparse Row format for the sparse matrices, and cuBLAS for GeMM with the Row Major format for the dense matrices. PIGO [11] is used for IO purposes. We use DGL 0.7.1 which is currently the latest available version [36]. We follow the instructions for compiling CAGNET [32] on its repository. For MG-GCN, we use NCCL (Nvidia Collective Communication Library) 2.11.4 and for CAGNET, we use NCCL 2.4.8 for compatibility reasons. The code for MG-GCN is available at <https://github.com/GT-TDAIab/MG-GCN>.

Datasets: We use two types of datasets in our experiment. The first category is GNN Benchmark datasets which are popular datasets used in GNN research, see Table 1. The Reddit dataset is a graph from Reddit posts that are posted in September, 2014 [15]. The node labels represent the communities (subreddits). Products (OGBN-Products) is a graph from Amazon co-purchase network. Nodes represents the products, and link represents products that are bought together. Proteins (OGBN-Proteins) is a biological network graph dataset where nodes represents proteins and edges represents associations between proteins. Arxiv (OGBN-Arxiv) and Cora are citation

networks where each node represent a paper and directed edges represent citation direction [16, 31].

Table 1: **Benchmark Datasets.** n : #vertices, m : #edges, $d^{(0)}$: #features, $d^{(L)}$: #classes, k : average degree.

DATASET	n	m	$d^{(0)}$	$d^{(L)}$	k
CORA	3.3K	9.2K	3.7K	6	3
ARXIV	169K	1.16M	128	40	7
PAPERS	111M	1.61B	128	172	15
PRODUCTS	2.5M	126M	104	47	52
PROTEINS	8.74M	1.3B	128	256	150
REDDIT	233K	115M	602	41	492

We also used synthetic datasets generated with BTER [22] to evaluate scalability of our method under varying density. BTER requires a degree distribution and clustering coefficient by degree as input and generates synthetic graphs matching those properties. We first profile the degree distribution of Arxiv dataset, then by increasing the average degree and fixing the number of vertices, we generate 8 synthetic datasets. We name these datasets as $1x, \dots, 128x$. As the name suggests, the number represents the scaling factor of number of edges from the original graph. We generate the features and assign class labels randomly. Each synthetic dataset has a feature vector of size 512, and there are 40 classes. Since the graphs generated by BTER are not deterministic, we generate 10 of each scale, and take the median while reporting the results.

Model: While we are able to train more complex models, to make fair comparisons, we use 4 different GCN models. First, to compare with CAGNET and DGL, we use a model with 2 layers, and the hidden layer consists of 512 neurons. Our limitation comes from the fact that, the available code for CAGNET does not have the option to change the number of layers. Second, to compare with DistGNN on Reddit, we use a model with 2 layers and hidden layer consists 16 neurons. To compare with DistGNN on Products, Protein and Papers, we use a model with 3 layers and hidden layers consist of 256 neurons. Finally, we use a 4th model with 3 layer, each consisting of 208 neurons to run MG-GCN on Papers DGX-A100, since 208 is the largest hidden layer size that can fit into DGX-A100. We have implemented and used the Adam optimizer [20] and the softmax cross entropy loss [7] in all of our experiments.

6.2 Runtime Breakdown of GCN Computation

We analyze the breakdown of execution time of GCN computation in order to find the computational bottlenecks during training. Figure 5 presents the runtime break-

down of the first GCN model described in Section 6.1. The activation layer refers to the computation in eq. (7), Adam refers to the update of the model parameters W by the Adam optimizer and loss layer refers to the computations related to the softmax cross entropy loss. As it is evident from the figure, for sufficiently large datasets, i.e., Proteins, Products, and Reddit, the main bottleneck is SpMM kernel which takes 60%-94% of the runtime, and second bottleneck is GeMM kernel 5%-20% of the runtime. On the other hand, for small datasets the main bottleneck becomes GeMM. Therefore, we stress the importance of parallelizing SpMM and GeMM kernels to achieve scalability during any GCN training, and focus our attention to parallelizing these kernels.

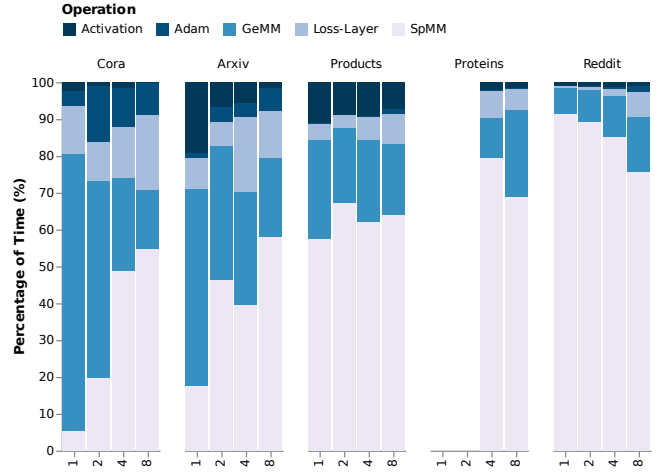


Figure 5: Runtime decomposition of operations involved in forward and backward pass.

6.3 Impact of Permutation

Figure 6 presents the breakdown of execution of SpMM to communication and computation times for each stage for the Product dataset using original and permuted ordering. On the top part of figure, there is a significant computational imbalance that hampers the efficient parallel execution. To remedy load imbalance problem we randomly permute the adjacency matrix before the computation. On the bottom part of the figure, permuted ordering achieves better computation load balance and reduces the execution time from 50ms to 38ms. Figure 7 shows normalized runtime improvement of permuted ordering w.r.t. original ordering for each dataset for varying number of GPUs. As seen in the figure, permutation yields slightly slower execution time on small number of GPUs for some dataset; however, as number of GPUs increases, the runtime improves significantly with the load balance achieved by permutation. For example, we observed $1.5\times$ runtime improvement on Products and Reddit datasets with 8 GPUs.

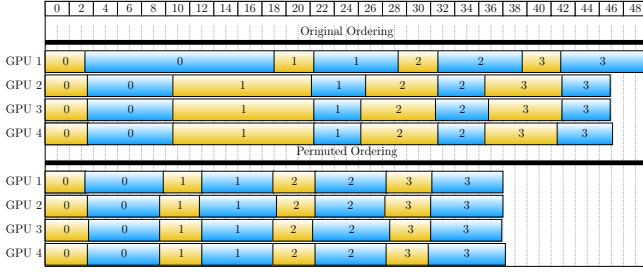


Figure 6: Timeline of the SpMM on the Products dataset using its original and permuted ordering. The numbers on the bars represent stages. For each GPU, computation (blue) and communication (yellow) phases are separately plotted.

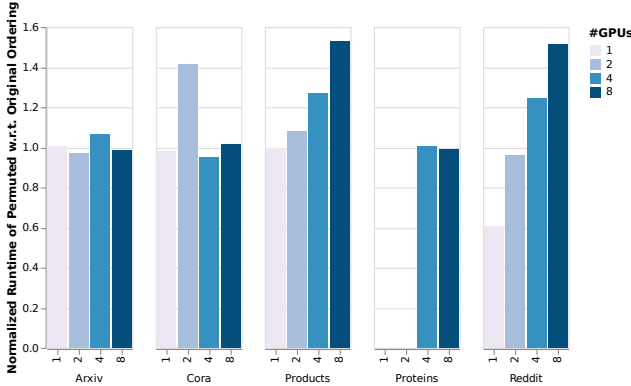


Figure 7: Effect of permuting to epoch runtime on DGX-V100.

6.4 Overlapping Computation and Communication

Figure 8 shows the effect of the communication-computation overlap on Products datasets using 4 GPUs. Notice that overlapping these two operations makes both the computation and the communication slower. This is because of the use of shared resources, in particular the memory bandwidth. Since SpMM is a mostly memory bandwidth bound operation, it becomes slower when overlapped with the communication kernel that takes up some of the global memory bandwidth. The global memory bandwidth of a V100 GPU is 900 GB/s and the communication bandwidth is 150 GB/s. Assuming the communication happens at full bandwidth, this results into a reduction of the global memory bandwidth for the SpMM operation by a factor of $\frac{1}{6}$. Nevertheless, communication-computation overlap still improves the performance. As seen in the figure, for Products, SpMM time can be reduced to 30ms from 38ms with overlapping communication and computation.

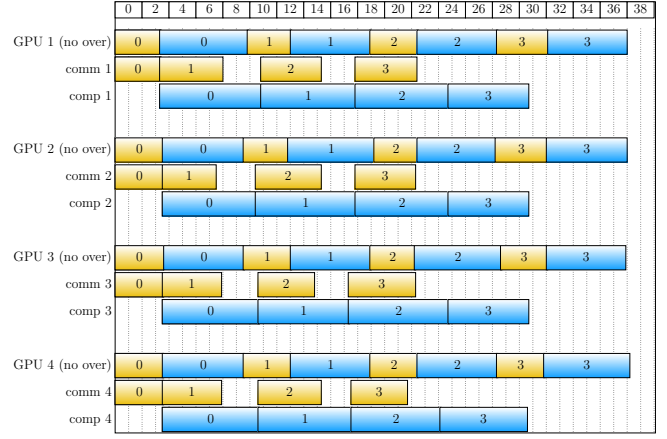


Figure 8: Timeline of the SpMM on the Products dataset using permuted ordering. The numbers on the bars represent stages. Each GPU is represented by 3 lines. First line represents computation without overlapping communication. Next two lines represent computation with overlapping communication. Blue line: computation time. Yellow line: communication time.

6.5 Impact of Average Degree

The runtime of SpMM can be mainly divided into two parts: computation time and communication time. Since we mostly overlap the two, the runtime can be at best maximum of those two. Communication time only depends on the dimensions of the matrix, whereas the computation time also depends on density and sparsity structure of the matrix. Furthermore, computation time starts to dominate the execution time as average degree increases. To illustrate the effect of this on speedup, we used the synthetic datasets generated by scaling the Arxiv dataset as explained in Section 6.1. Figure 9 displays the speedups obtained by 2 to 8 GPUs, while we increase the average degree. As seen in the figure, our code starts to achieve super-linear speedup with 2 and 4 GPUs, after $32\times$, and with 8 GPUs, after $64\times$ scaling. We attribute this super-linear speedup numbers for very dense adjacency matrices because of the blocking effect of partitioning and potentially better use of the cache.

6.6 Comparison on Single Node Systems

Comparison on DGX-V100: In Figures 10 and 11, we compare MG-GCN with DGL and CAGNET using the 2 layer model mentioned in Section 6.1 on DGX-V100. Note that, CAGNET has different partitioning strategies namely, 1D, 1.5D, 2D and 3D. We present the best results which are produced by 1D partitioning. In all datasets, we outperform DGL with a single GPU and CAGNET with multiple GPUs. Our single GPU performances are, $2.72\times$ faster on Reddit, $1.42\times$ faster on Products, $1.76\times$ faster on Arxiv and $3.1\times$ faster on Cora than DGL. Our 8 GPU performances are $2.66\times$ faster on Reddit, $8.6\times$

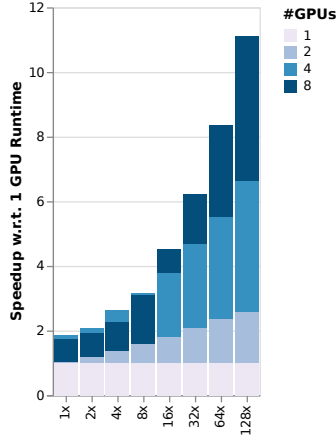


Figure 9: Speedup w.r.t. MG-GCN 1 GPU Runtime

faster on Products, $2.35\times$ faster on Arxiv than CAGNET. Notice that, neither MG-GCN or CAGNET is able to get a speedup on Cora dataset, since the graph is very small and certain amount of work is expected to achieve any speedup. We are not able to run CAGNET with Proteins dataset using 8 GPUs because of CAGNET’s memory requirement; however, MG-GCN is able to fit Proteins dataset into 4 only GPUs. Even though, both CAGNET and MG-GCN use 1D partitioning, we are able to fit much larger graphs into our target machines due to extensive memory optimization described in Section 4.2. Also, by overlapping computation and communication, we achieve substantial speedup compared to CAGNET.

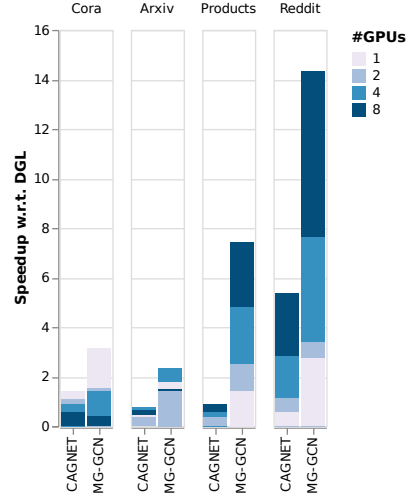


Figure 11: Speedup w.r.t. DGL on DGX-V100.

it is not compatible with CUDA 11. In all the datasets, we outperform DGL with a single GPU. Our single GPU results are $2.2\times$ faster on Cora, $1.8\times$ faster on Arxiv, $1.5\times$ faster on Products and $1.5\times$ faster on Reddit datasets than DGL. On multi-GPU setting, MG-GCN is able to achieve $8.5\times$ speedup on Products dataset, and $8.3\times$ speedup on Reddit dataset using 8 GPUs. Moreover, we are able to fit Papers dataset, which is the largest available benchmark dataset for GNN training, into 8 GPUs with MG-GCN, and achieve 2.89 seconds epoch runtime using the 4th GCN model mentioned in Section 6.1.

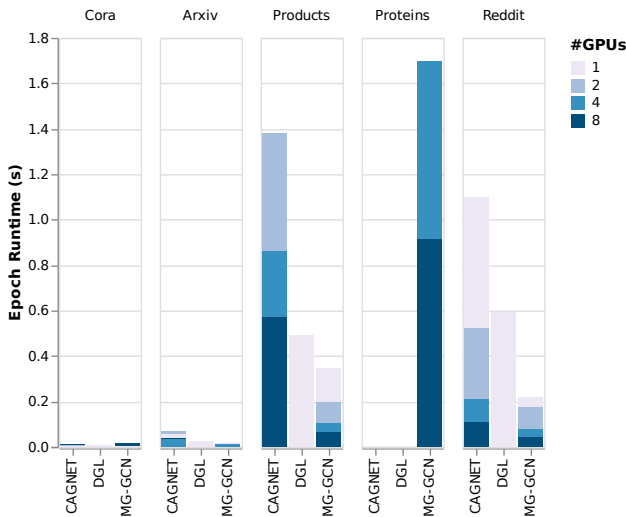


Figure 10: Baseline epoch runtime (seconds) comparison on DGX-V100. On Proteins dataset CAGNET and DGL run out of memory, MG-GCN runs out of memory with 1 and 2 GPUs.

Comparison on DGX-A100: In Figures 12 and 13, we compare MG-GCN with DGL using the 2 layer GCN model mentioned in Section 6.1 on DGX-A100. We are not able to include CAGNET in this comparison, since

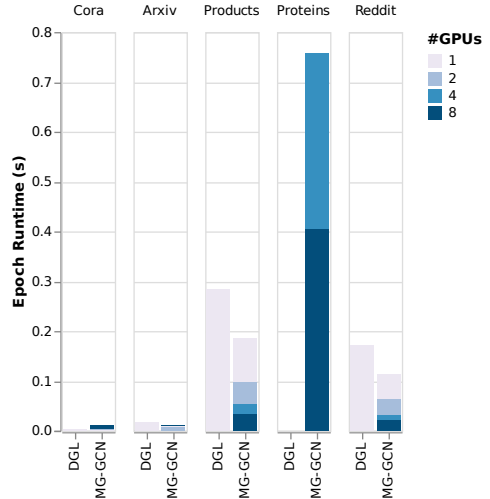


Figure 12: Epoch runtime (seconds) comparison on DGX-A100.

6.7 Single Node vs Distributed Systems

We compare MG-GCN with DistGNN using 2 different GCN models mentioned in section 6.1. Note that, this is not an exact comparison for two main reasons: First, we are not able reproduce the results because the source code

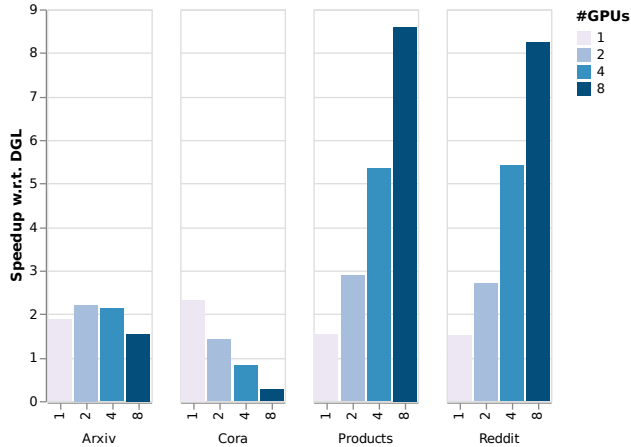


Figure 13: Speedup w.r.t. DGL on DGX-A100.

of DistGNN is not available, so we base our comparison to the numbers reported in the original work. Second, DistGNN is a CPU based framework, while MG-GCN is designed for GPUs. We believe that, comparing the two frameworks will provide important insights on the resource requirements and performance one can get. For the experiments, DistGNN uses a cluster with 64 Intel Xeon 9242 CPU @2.30 GHz with 48 cores per socket in a dual-socket system. The compute nodes consist of 384 GB memory, and connected through Mellanox HDR interconnect with DragonFly topology. In addition, to run Papers on a single socket, they use a single-socket machine with 1.5TB memory.

Table 2 shows the results from DistGNN, while Table 3 shows the performance of MG-GCN on DGX-A100. In Table 2, we only take the single socket and the best socket performances for each dataset from the original work [27]. Also, note that, we compare against their baseline version, since other variants are not exact computations but approximations. For detailed results, we refer interested readers to [27]. Even though, the authors observe significant speedups in their experiments, MG-GCN outperforms their best performance with a single GPU on all datasets except Proteins. Our 8 GPU performances are $40\times$ faster on Reddit, $12.6\times$ faster on Papers, $12.4\times$ faster on Products, and $1.77\times$ faster on Protein datasets than DistGNN’s best performances. Note that, for Reddit dataset, since the GCN model is very small, 2 layers with 16 neurons, MG-GCN cannot achieve speedup after 4 GPUs.

7 Conclusion

In this paper, we present MG-GCN, a single node multi-GPU GCN training framework which enables efficient distributed training of GCNs over the full-graph. MG-GCN adapts a 1D row partitioning strategy. It also adapts extensive memory optimizations by re-using/sharing the allocated buffers across layers and forward/backward

Table 2: **DistGNN Results:** The numbers in the cells are epoch times in second. For each dataset, we take results for 1 Socket and the number of sockets that performs the best from [41]. DS: Dataset, #S: Number of Sockets.

DS #S	REDDIT	PAPERS	PRODUCTS	PROTEIN
1	0.60	1000	11	100
16	0.61	-	-	-
64	-	-	1.74	2.63
128	-	36.45	-	-

Table 3: **MG-GCN Results on DGX-A100:** The values in the cells are epoch times in seconds. Dashed line represents configurations that run out of memory. DS: Dataset, #G: Number of GPUs.

DS #G	REDDIT	PAPERS	PRODUCTS	PROTEIN
1	0.033	-	0.355	4.221
2	0.017	-	0.202	2.272
4	0.012	-	0.110	1.191
8	0.012	2.89	0.067	0.641

phases, and enables overlapping communication and computation. We have demonstrated that, MG-GCN is able to achieve significant runtime improvements over the available state-of-the-art frameworks on single GPU systems. Moreover, going into the multi-GPU setting, we are able to fit much larger graphs into the memory of our target machines. In our single GPU experiments, we achieve up-to $2.72\times$ speedup compared to DGL on Reddit dataset, and on multi-GPU experiments we achieve up-to $8.6\times$ speedup on Products dataset compared to CAGNET on DGX-V100.

In future work, we are aiming to extend our framework to multi-GPU clusters. By doing so, we aim to train larger datasets and enable distributed training of even larger scale GNNs. Another future direction is to accelerate the Sampled Dense Dense Matrix Multiplication (SDDMM) kernel to enable parallel training of a number of other models such as Graph Attention Networks [34].

8 Acknowledgements

We thank Prof. Polo Chau for providing us access to their DGX-A100 for our experiments. This work was partially supported by the NSF grant CCF-1919021.

References

- [1] Martín Abadi, Ashish Agarwal, Paul Barham, Eugene Brevdo, Zhifeng Chen, Craig Citro, Greg S. Corrado, Andy Davis, Jeffrey Dean, Matthieu Devin, Sanjay Ghemawat, Ian Goodfellow, Andrew Harp, Geoffrey Irving, Michael Isard, Rafal Jozefowicz, Yangqing Jia, Lukasz Kaiser, Manjunath Kudlur, Josh Levenberg, Dan Mané, Mike Schuster, Rajat Monga, Sherry Moore, Derek Murray, Chris Olah, Jonathon Shlens, Benoit Steiner, Ilya Sutskever, Kunal Talwar, Paul Tucker, Vincent Vanhoucke, Vijay Vasudevan, Fernanda Viégas, Oriol Vinyals, Pete Warden, Martin Wattenberg, Martin Wicke, Yuan Yu, and Xiaoqiang Zheng. Tensorflow, October 2021.
- [2] Tal Ben-Nun and Torsten Hoefer. Demystifying parallel and distributed deep learning: An in-depth concurrency analysis. *ACM Computing Surveys (CSUR)*, 52(4):1–43, 2019.
- [3] Jie Chen, Tengfei Ma, and Cao Xiao. FastGCN: Fast learning with graph convolutional networks via importance sampling. In *International Conference on Learning Representations*, 2018.
- [4] Tianqi Chen, Mu Li, Yutian Li, Min Lin, Naiyan Wang, Minjie Wang, Tianjun Xiao, Bing Xu, Chiyuan Zhang, and Zheng Zhang. Mxnet: A flexible and efficient machine learning library for heterogeneous distributed systems, 2015.
- [5] Wei-Lin Chiang, Xuanqing Liu, Si Si, Yang Li, Samy Bengio, and Cho-Jui Hsieh. Cluster-gcn: An efficient algorithm for training deep and large graph convolutional networks. In *Proceedings of the 25th ACM SIGKDD International Conference on Knowledge Discovery & Data Mining*, pages 257–266, 2019.
- [6] Adam Coates, Brody Huval, Tao Wang, David Wu, Bryan Catanzaro, and Ng Andrew. Deep learning with cots hpc systems. In *International conference on machine learning*, pages 1337–1345. PMLR, 2013.
- [7] D. R. Cox. The regression analysis of binary sequences. *Journal of the Royal Statistical Society. Series B (Methodological)*, 20(2):215–242, 1958.
- [8] Li Deng, Dong Yu, and John Platt. Scalable stacking and learning for building deep architectures. In *2012 IEEE International Conference on Acoustics, Speech and Signal Processing (ICASSP)*, pages 2133–2136, 2012.
- [9] Ludvig Ericson and Rendani Mbuyha. On the performance of network parallel training in artificial neural networks. *arXiv preprint arXiv:1701.05130*, 2017.
- [10] Matthias Fey and Jan E. Lenssen. Fast graph representation learning with PyTorch Geometric. In *ICLR Workshop on Representation Learning on Graphs and Manifolds*, 2019.
- [11] Kasimir Gabert and Ümit V. Çatalyürek. PIGO: A parallel graph input/output library. In *2021 IEEE International Parallel and Distributed Processing Symposium Workshops (IPDPSW)*, pages 276–279. IEEE, 2021.
- [12] Boris Ginsburg, Igor Gitman, and Yang You. Large batch training of convolutional networks with layer-wise adaptive rate scaling, 2018.
- [13] Joseph E. Gonzalez, Yucheng Low, Haijie Gu, Danny Bickson, and Carlos Guestrin. Powergraph: Distributed graph-parallel computation on natural graphs. In *Proceedings of the 10th USENIX Conference on Operating Systems Design and Implementation, OSDI’12*, page 17–30. USENIX Association, 2012.
- [14] Priya Goyal, Piotr Dollár, Ross Girshick, Pieter Noordhuis, Lukasz Wesolowski, Aapo Kyrola, Andrew Tulloch, Yangqing Jia, and Kaiming He. Accurate, large minibatch sgd: Training imagenet in 1 hour. *arXiv preprint arXiv:1706.02677*, 2017.
- [15] William L. Hamilton, Rex Ying, and Jure Leskovec. Inductive representation learning on large graphs, 2018.
- [16] Weihua Hu, Matthias Fey, Marinka Zitnik, Yuxiao Dong, Hongyu Ren, Bowen Liu, Michele Catasta, and Jure Leskovec. Open graph benchmark: Datasets for machine learning on graphs, 2021.
- [17] Zhihao Jia, Sina Lin, Mingyu Gao, Matei Zaharia, and Alex Aiken. Improving the accuracy, scalability, and performance of graph neural networks with roc. *Proceedings of Machine Learning and Systems (MLSys)*, pages 187–198, 2020.
- [18] Peng Jiang, Changwan Hong, and Gagan Agrawal. A novel data transformation and execution strategy for accelerating sparse matrix multiplication on GPUs. In *Proceedings of the 25th ACM SIGPLAN Symposium on Principles and Practice of Parallel Programming, PPOPP ’20*, page 376–388. Association for Computing Machinery, 2020.
- [19] George Karypis and Vipin Kumar. A fast and high quality multilevel scheme for partitioning irregular graphs. *SIAM Journal on Scientific Computing*, 20:359–392, 1998.
- [20] Diederik P. Kingma and Jimmy Ba. Adam: A method for stochastic optimization, 2017.
- [21] Thomas N. Kipf and Max Welling. Semi-supervised classification with graph convolutional networks. In

- 5th International Conference on Learning Representations, ICLR 2017, Toulon, France, April 24-26, 2017, Conference Track Proceedings. OpenReview.net, 2017.
- [22] Tamara G. Kolda, Ali Pinar, Todd Plantenga, and C. Seshadhri. A scalable generative graph model with community structure. *SIAM Journal on Scientific Computing*, 36(5):C424–C452, Jan 2014.
- [23] Alex Krizhevsky. One weird trick for parallelizing convolutional neural networks. *arXiv preprint arXiv:1404.5997*, 2014.
- [24] Y. Lecun, L. Bottou, Y. Bengio, and P. Haffner. Gradient-based learning applied to document recognition. *Proceedings of the IEEE*, 86(11):2278–2324, 1998.
- [25] Ang Li, Shuaiwen Leon Song, Jieyang Chen, Jiajia Li, Xu Liu, Nathan R. Tallent, and Kevin J. Barker. Evaluating modern GPU interconnect: PCIe, NVLink, NV-SLI, NVSwitch and GPUDirect. *IEEE Transactions on Parallel and Distributed Systems*, 31(1):94–110, Jan 2020.
- [26] Lingxiao Ma, Zhi Yang, Youshan Miao, Jilong Xue, Ming Wu, Lidong Zhou, and Yafei Dai. Neugraph: Parallel deep neural network computation on large graphs. In *2019 USENIX Annual Technical Conference (USENIX ATC 19)*, pages 443–458. USENIX Association, July 2019.
- [27] Vasimuddin Md, Sanchit Misra, Guixiang Ma, Ramnarayan Mohanty, Evangelos Georganas, Alexander Heinecke, Dhiraj Kalamkar, Nesreen K Ahmed, and Sasikanth Avancha. Distgcn: Scalable distributed training for large-scale graph neural networks. *arXiv preprint arXiv:2104.06700*, 2021.
- [28] Vinod Nair and Geoffrey E. Hinton. Rectified linear units improve restricted boltzmann machines. In *Proceedings of the 27th International Conference on International Conference on Machine Learning, ICML’10*, page 807–814, Madison, WI, USA, 2010. Omnipress.
- [29] Adam Paszke, Sam Gross, Francisco Massa, Adam Lerer, James Bradbury, Gregory Chanan, Trevor Killeen, Zeming Lin, Natalia Gimelshein, Luca Antiga, Alban Desmaison, Andreas Kopf, Edward Yang, Zachary DeVito, Martin Raison, Alykhan Tejani, Sasank Chilamkurthy, Benoit Steiner, Lu Fang, Junjie Bai, and Soumith Chintala. Pytorch: An imperative style, high-performance deep learning library. In H. Wallach, H. Larochelle, A. Beygelzimer, F. d’Alché-Buc, E. Fox, and R. Garnett, editors, *Advances in Neural Information Processing Systems 32*, pages 8024–8035. Curran Associates, Inc., 2019.
- [30] Franco Scarselli, Marco Gori, Ah Chung Tsoi, Markus Hagenbuchner, and Gabriele Monfardini. The graph neural network model. *IEEE Transactions on Neural Networks*, 20(1):61–80, 2009.
- [31] Prithviraj Sen, Galileo Mark Namata, Mustafa Bilgic, Lise Getoor, Brian Gallagher, and Tina Eliassi-Rad. Collective classification in network data. *AI Magazine*, 29(3):93–106, 2008.
- [32] Alok Tripathy, Katherine A. Yelick, and Aydin Buluç. Reducing communication in graph neural network training. *CoRR*, abs/2005.03300, 2020.
- [33] Robert A. van de Geijn and Jerrell Watts. Summa: scalable universal matrix multiplication algorithm. *Concurr. Pract. Exp.*, 9:255–274, 1997.
- [34] Petar Veličković, Guillem Cucurull, Arantxa Casanova, Adriana Romero, Pietro Liò, and Yoshua Bengio. Graph attention networks, 2018.
- [35] Minjie Wang, Da Zheng, Zi-Hao Ye, Q. Gan, Mufei Li, Xiang Song, Jinjing Zhou, Chao Ma, Lingfan Yu, Yu Gai, Tianjun Xiao, Tong He, G. Karypis, Jinyang Li, and Zheng Zhang. Deep graph library: A graph-centric, highly-performant package for graph neural networks. 2019.
- [36] Minjie Wang, Da Zheng, Zihao Ye, Quan Gan, Mufei Li, Xiang Song, Jinjing Zhou, Chao Ma, Lingfan Yu, Yu Gai, Tianjun Xiao, Tong He, George Karypis, Jinyang Li, and Zheng Zhang. Deep graph library: A graph-centric, highly-performant package for graph neural networks. *arXiv preprint arXiv:1909.01315*, 2019.
- [37] Cong Xie, Ling Yan, Wu-Jun Li, and Zhihua Zhang. Distributed power-law graph computing: Theoretical and empirical analysis. In *Advances in Neural Information Processing Systems*, volume 27. Curran Associates, Inc., 2014.
- [38] Kunlei Zhang and Xue-Wen Chen. Large-scale deep belief nets with mapreduce. *IEEE Access*, 2:395–403, 2014.
- [39] Muhan Zhang and Yixin Chen. Link prediction based on graph neural networks. *Advances in Neural Information Processing Systems*, 31:5165–5175, 2018.
- [40] Muhan Zhang, Zhicheng Cui, Marion Neumann, and Yixin Chen. An end-to-end deep learning architecture for graph classification. In *Thirty-Second AAAI Conference on Artificial Intelligence*, 2018.
- [41] Da Zheng, Chao Ma, Minjie Wang, Jinjing Zhou, Qidong Su, Xiang Song, Quan Gan, Zheng Zhang, and George Karypis. Distdgl: distributed graph neural network training for billion-scale graphs. In

2020 IEEE/ACM 10th Workshop on Irregular Applications: Architectures and Algorithms (IA3), pages 36–44. IEEE, 2020.

- [42] Rong Zhu, Kun Zhao, Hongxia Yang, Wei Lin, Chang Zhou, Baole Ai, Yong Li, and Jingren Zhou. Ali-graph: A comprehensive graph neural network platform. *Proc. VLDB Endow.*, 12(12):2094–2105, August 2019.
- [43] Martin Zinkevich, Markus Weimer, Alexander J Smola, and Lihong Li. Parallelized stochastic gradient descent. In *NIPS*, volume 4, page 4. Citeseer, 2010.